NATIONAL INSTITUTE OF AEROSPACE

Final Report For
The Creation of a Physics-Based Ground-Effect Model, Phase 2 - Inclusion of the effects of Wind, Stratisfication, and Shear into the New Ground Effect Model

NASA TASK ORDER NUMBER NNL06AB77T
TM: Wayne Bryant

Prepared By: Dr. Sarpkaya

HYDRODYNAMIC APPLICATIONS INC.

FINAL TECHNICAL REPORT

A Physics-based Real-time IGE model of Aircraft Wake Vortices Subjected to crosswind and Stratification

Executive Summary

The reduction of the separation of the leading and following aircrafts is desirable to enhance the airport capacity provided that there is a physics-based operational model applicable to all regions of the flight domain (out of ground effect, OGE; near ground effect, NGE; and in ground effect, IGE) and that the quality of the quantitative input from the measurements of the prevailing atmospheric conditions and the quality of the total airport operations regarding the safety and the sound interpretation of the prevailing conditions match the quality of the analysis and numerical simulations. In the absence of an analytical solution, the physics of the flow is best expressed by a mathematical model based on numerical simulations, field and laboratory experiments, and heuristic reasoning. T*his report deals with the creation of a sound physics-based real-time IGE model* of the aircraft wake vortices subjected to crosswind, stratification and shear. The performance of the model is assessed through the use of an LES simulation by Proctor, *et al.* (2000), and the field measurements: MEM-1576, MEM-1500, MEM-1494, and IDAHO-757 Run 9. The comparison of the model predictions with additional Large Eddy Simulations (LES) and with the existing as well as new field data using larger aircraft requires further work to render the model fully operational.

Dr. T. Sarpkaya

Senior Research Scientist and CEO,

Hydrodynamic Applications, Inc.

NIA Subcontract No: TO6-6000-HAI

Placed under NASA Prime Contract No: NAS1-02117

1 October 2006

TABLE OF CENTENTS

LIST OF ILLUSTRATIONS

LIST OF SYMBOLS

B = aircraft wing span

b_o = initial vortex separation - $\pi B/4$

L = denotes left

R = denotes right

r = radius from vortex center

Sh_p = shear parameter: $(b_o/V_{sv})(dV_{sv}/dz)$

t = time coordinate

T = nondimensional time – $V_o\, t/b_o$

T_G = T at $z = z_{min}$

V_a = airspeed of generating aircraft

V_o = initial vortex descent velocity: $\Gamma_o/(2\pi b_o)$

V_s = slip velocity

V_{sv} = shear velocity

Z_{bl} = boundary layer thickness

v = transport component of the vortex in the y (lateral) direction

w = transport component of the vortex in the z (vertical) direction

Y = y/b_o, lateral coordinate

Z = z/b_o, vertical coordinate

Z_{bl} = boundary layer thickness

Γ = vortex circulation

Γ_o = initial vortex circulation

$\alpha, \beta, \kappa, \lambda$ = uncertainty parameters (all near unity)

δ = boundary layer thickness

δ_1 = displacement thickness

ν = kinematic viscosity

ACKNOWLEDGMENTS

This research was sponsored by NASA's Airspace Systems/Airportal Program and managed by NIA. Special thanks are extended to Dr. Fred H. Proctor of the Aviation Operations and Evaluation Branch (D323), the **Technical Manager** of this project, for providing much inspiration through the years. The continued support and encouragement of Dr. Wayne H. Bryant (NASA, Larc) are gratefully acknowledged.

The ever willing and generous support of Ms. Crystal M. Glenn and Ms. Gwen Wessen of the National Institute of Aerospace are sincerely appreciated.

INTRODUCTION

The development of a physics-based real-time *Ground Effect* prediction model depends on the aircraft, on a clear understanding of the characteristics of the resulting vortices, atmospheric input (most importantly crosswind and stratification), and the prevailing unsteady, turbulent boundary layers on the ground. These affect not only the trajectory of the vortices but also the friction and pressure signals along the wall. Thus, the IGE defines one of the most complex time-dependent flows in fluid dynamics. The existing In-Ground-Effect (IGE) models (or approximations) are based on the use of a large number of particles (to mimic the field tests) or on curve fitting through the use of more-or-less arbitrary *circulation reductions*. Clearly, curve fitting is not an option and is not in conformity with the new directions of NASA towards the *fundamentals*. Nevertheless, these efforts (mostly for flights out of ground effect) led to fairly satisfactory comparisons between the model predictions and the generating aircraft, but lacked physics and reliability. The clearest understanding of the IGE came not so much from field tests (at best, difficult to perform) or from low-Reynolds number laboratory experiments (small-scale, sometimes misleading) but rather from the 3-D LES simulations [Proctor & Han (1999), Proctor, Hamilton, & Switzer (2006)]. In these studies, the effects of windshear were not considered. The numerical solutions such as these, however valuable, cannot, and are not expected to cover the entire parameter space; they only serve as inspiration for the creation of real-time models.

Low-Reynolds-number experiments often and inadvertently convey the impression that the results and conclusions are valid at all Reynolds numbers. With vortical flows, in a highly complex atmospheric environment, one cannot expect to extract correct physics from laminar flow experiments for a number of reasons, the most important ones being the boundary layers on the ground and the diffusion of vorticity (shortly after the creation of the vortices) which are turbulent to varying degrees of scale and intensity. To make a clear distinction, we refer hear not to the commonly used expression of “vortex decay”

but rather to the "often turbulent and rarely laminar diffusion" of vorticity and its annihilation in the overlapping regions of "oppositely signed vorticity". This is akin to but not identical to the interaction of a trailing vortex pair with an embedded and often nonlinear (or three-dimensional) ambient shear. In view of the foregoing, we have undertaken an in-depth review of some of the more notable contributions.

BRIEF REVIEWS OF THE PREVIOUS CONTRIBUTIONS

(A) Suponitsky, Cohen, & Bar-Yoseph (2004) have shown that when an unbounded uniform shear interacts with a vortex element (e.g., a vortex ring), the streamwise and spanwise distributions of vorticity for the viscous and inviscid cases are identical. Once the disturbance is sufficiently large, the shape of the vorticity distribution is well preserved by the inviscid solution, but its actual magnitude is severely overestimated. Throughout the interaction of the uniform shear with the vortex element (here a vortex ring), the shape of the vortex element changes dramatically (from a circular to a U-shaped horseshoe vortex, see figure 1, below). *It follows that it is not the initial shape of the shear layer or its extent, but rather the disregarding of the effects of viscosity and the interactive deformations of the shear layer and the vortex elements that lead to erroneous results and conclusions.*

The figure 1 shows the deformations of a vortex ring. If the shear layers are considered as composed of *non-deformable beads on a flexible string and the cores of the vortices non-deformable* (with no interference by viscosity/turbulence) then and only then one can show that linear shear does not affect the shape and the motion of the non-deformable vortex. Such an analysis may not be acceptable for the prediction of rebound (depending on how the strengths of the vortices are made a function of time). In other words, it is important to note that the consequences of the interaction of either a laminar (linear or nonlinear) shear or a turbulent (linear or nonlinear) shear, bounded or

unbounded, with a non-deformable vortex (in lieu of a real deformable vortex) are far too complex and incalculable simply because the correct physics is missing. Transient growth and deformation in the presence of viscosity and turbulence are the integral ingredients of the analysis and the understanding of the consequences of shear on rebound through the use of *physics-based analysis tools*.

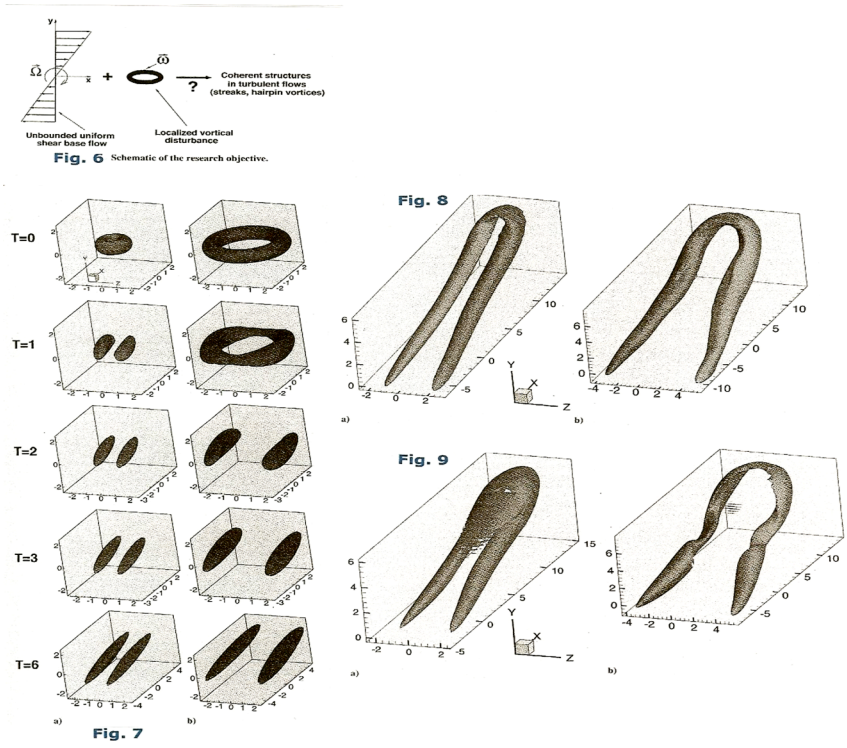

Figure 1. Deformation of a vortex ring in uniform shear.

Suponitsky, Cohen & Bar-Yoseph (2004).

(B) Hofbauer & Gerz (1999) dealt with the influence of nonlinear vertical shear on the trajectories of a trailing vortex pair. They have considered shear layers where the velocity increases monotonically from one constant value to another within a given

height interval, as shown in Fig. 2. Their second case is the shear layers in the form of low-level jets as often observed in early morning boundary layers.

The numerical model used by Hofbauer & Gerz (1999) is the full set of N-S equations in their conservative form for an incompressible fluid. The simulations are initialized by the linear superposition of two counter-rotating Lamb-Oseen-vortices with circulations of 25 m^2/s and b_o = 24 m. It is important to note that dotted contours denote negative vorticity (i.e., the vortex is rotating in the CCW direction). Clearly, the primary vortices descend due to their mutual induction and while being advected by the prevailing crosswind. They have concluded that "*the shear layer strength in terms of shear layer circulation per unit length is no comprehensive measure for the rebounce phenomenon*."

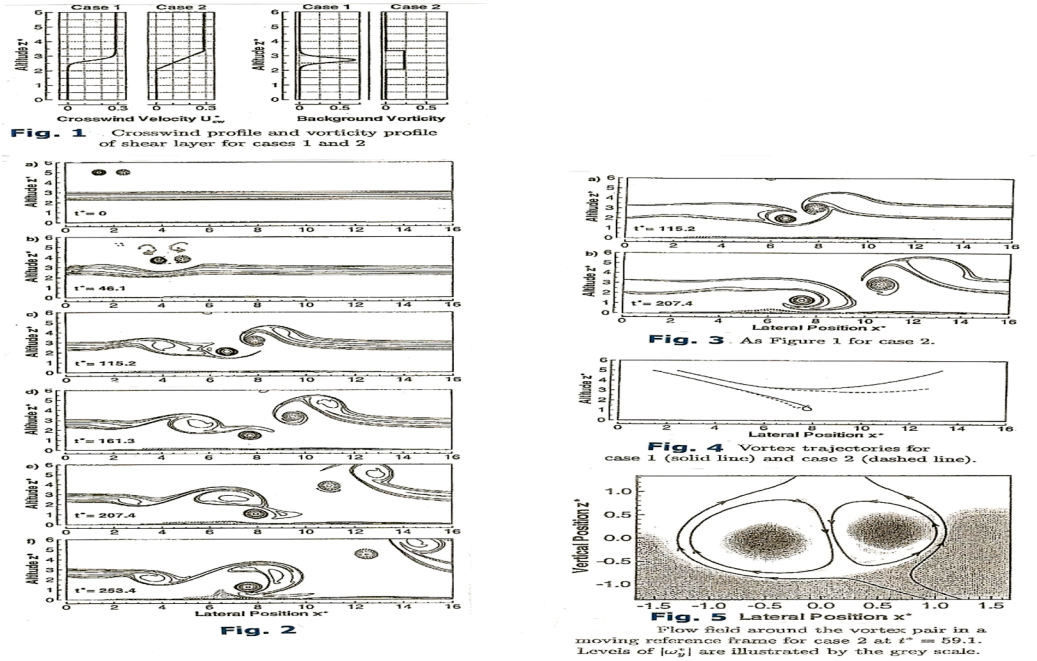

Figure 2. Effects of nonlinear shear on the dynamics of a counter-rotating vortex pair Hofbauer & Gerz (1999).

The authors suggested that the maximum of the vorticity of the shear-layer and the shear-layer thickness might be the most relevant parameters. They have also correctly

concluded that "the vorticity of each discrete infinitesimal area of the shear layer induces an infinitesimal velocity on the primary vortices according to the Biot-Savart law." Since the effect of velocity induction decreases with distance, the shear layer deformation causes different induced velocities for the upwind and downwind vortex, which explains their differing trajectories.

It is apparent from the foregoing two studies that:

(a) shear layers may cause descending vortices to stall or even to rise;

(b) vortex-pair tilting and divergence are integral parts of the rebound;

(c) the vortex whose vorticity is of opposite sign to that of the shear layer is more likely to rebound and to demise sooner;

(d) the rebound may also be affected by the distribution of shear within the shear layer;

(e) The three-dimensional nature of the phenomenon may have further consequences on rebound;

(f) The use of a few vortices and shear-layer elements for the analysis of the evolution of aircraft wake-vortices in ground effect is at best 'curve fitting' by trial and error. Only 3-D LES simulations (e.g., Proctor, Hinton, Han, Schowalter, & Lin (1997) can provide reliable and intelligent guidance to physics-based modeling of rebound (*clearly more of such simulations are urgently needed*). The model has to be valid for a large domain of the controlling as well as influencing variables (atmospheric, aircraft wake, airport, etc.), approximate enough but not too approximate so as not to violate the physics of the phenomenon and the known or already discovered facts, improvable, and operational so as to provide predictions in real time. Thus, *the creation of a physics-based real-time model is far more complex than either the experiments or the numerical simulations.*

Real vortex-pair flows are often inadequately characterized by the classical point vortex-pair models. A more realistic model considers the steady motion of an *asymmetric*, finite core size, counter-rotating vortex pair in an unbounded domain. The

vortices are characterized by their circulations, centroid-to-centroid spacing, and translational velocities (not necessarily identical). Often the vorticity inside the vortices is assumed to be uniformly distributed. However, in real vortices (particularly those in shear) the vorticity is not uniformly distributed and the density of the vorticity distribution changes with the evolution of the vortices interacting with other vortices (e.g., images). Unfortunately, not all of these details can be incorporated into a model. However, the evolutionary creation of a physics-based model requires total awareness of all the real and imaginable facts and variables, the ability to sort out the primary controlling parameters from among all those that come into one's attention span, and the gift of quickly transforming the essence of these facts into analytical expressions.

The unending search for a fast forecasting algorithm for the shear-vortex interaction led to the use of numerous approximate models. Some use a large number of discrete vortices (with all of their limitations due to the 1/r relationship in the Biot-Savart law) and *the arbitrariness of the diffusion and annihilation of vorticity*. The ambient shear is modeled in the same manner. Often the decay of circulation is neglected or approximated and the major role played by the ground and the boundary conditions is ignored (except in defining the positions of the image vortices!).

(C) Robins & Delisi (2006) introduced the crosswind shear effects into the AVOSS prediction algorithm through the use of a highly simplified and questionable model. In short, the circulation of the vortex oval (assuming that there is still a vortex oval by the time the vortices reach NGE and IGE regions) is calculated at any given time by augmenting the prevailing circulation with two additional terms. The first is the *decay rate of circulation* (due to environmental factors such as turbulence and stratification) times the time interval Δt; the second is the *decay rate of circulation due to shear effects*, guesstimated at every time step in the Near Ground Effect region by going *one step backward and two steps forward*. It must be emphasized that "the decay rate of circulation (due to environmental factors such as turbulence and stratification" is extremely complex and directly related to the diffusion and decay of vorticity on the

ground." Thus, Robins & Delisi's (2006) so-called '*predictive mode*' and '*diagnostic mode*' are at best curve fitting (or circulation fitting) to the field measurements. They have noted that "to run the algorithm iteratively, varying the crosswind profile and the circulation history in a systematic way, until the computed vortex trajectories agree with the measured trajectories." They have suggested that "A possible future direction based on these results is to develop a *prediction model* that continuously updates the crosswind profile and uses a simple decay formulation for circulation." This is what we meant by "*going one step backward and two steps forward with no acceptable reason."* Therefore, it is not meaningful to talk about "a simple decay formulation for circulation" because it is anything but simple. This type of curve-fitting approach (used in the mid 90's) does not enhance the state of the art. *It is therefore important that all approaches to IGE modeling must be taken to a higher ground. This is the only way NASA can advance the state of the art and the power of prediction in this branch of aerodynamics.*

(D) The numerical simulations of Hofbauer & Holzäpfel (2003) have suggested that "neither the local shear rate nor its rate of change is suitable for quantifying vortex rebound". "However, using the wind speed U(z) permits a good estimation for the lateral vortex transport out of ground. As far as the expended parameter space is concerned, it is not obvious what the most important parameters are." The inspiration might come from numerical simulations if one can afford to carry out numerous simulations with carefully chosen values for the parameter-space used. Experiments are likely to provide better guidance in spite of their often-stated shortcomings provided that they are carried at *sufficiently high Reynolds numbers (circulation/kinematic viscosity).* It is a well-known fact that major loss of vorticity occurs on and very near the ground and its accurate prediction is of great importance as far as an operational model is concerned.

(E) Zheng and Baek (1998) examined the *inviscid* interactions between two oppositely-signed vortices of constant strength with a horizontal shear layer of finite thickness (comprised of smaller identical vortices of same sign and constant strength),

below or above the vortex pair. This work was motivated by the computational work of Proctor *et al.* (1997) on the effects of narrow shear zones on the behavior of a vortex pair. Zheng and Baek (1998) have shown that the downwind vortex is more sensitive and deflected to a higher altitude than its upwind counterpart.

(F) As noted earlier, only 3-D LES simulations [e.g., Proctor *et al.* (1997)] can provide reliable and intelligent guidance to physics based modeling of rebound (*clearly more of such simulations are urgently needed*) in view of the fact that *the creation of a physics-based real-time model is far more complex than either the experiments or the numerical simulations.*

A PHYSICS BASED IGE MODEL (no shear)

As noted by Sarpkaya (2006), [see also Sarpkaya 2000 & 2004)], the model is based on the following physical facts:

(i) The spanwise component of the oppositely-signed wall shear stress (due to zero slip, zero penetration condition) gives rise to a torque retarding the rotation of each vortex (or decreasing its circulation);

(ii) each vortex creates a boundary layer (and, hence, a displacement thickness) which shifts the external streamlines by δ_1; and

(iii) the vortices, highly decayed by the oppositely-signed vorticity generated on the ground over a time period T, are left in the hands of the prevailing atmospheric conditions to eventually become puffy incoherent structures.

Two oppositely signed vortices of unequal strength (and their images) are considered and it is assumed that the reader is facing the aircraft, as shown in Fig. 3.

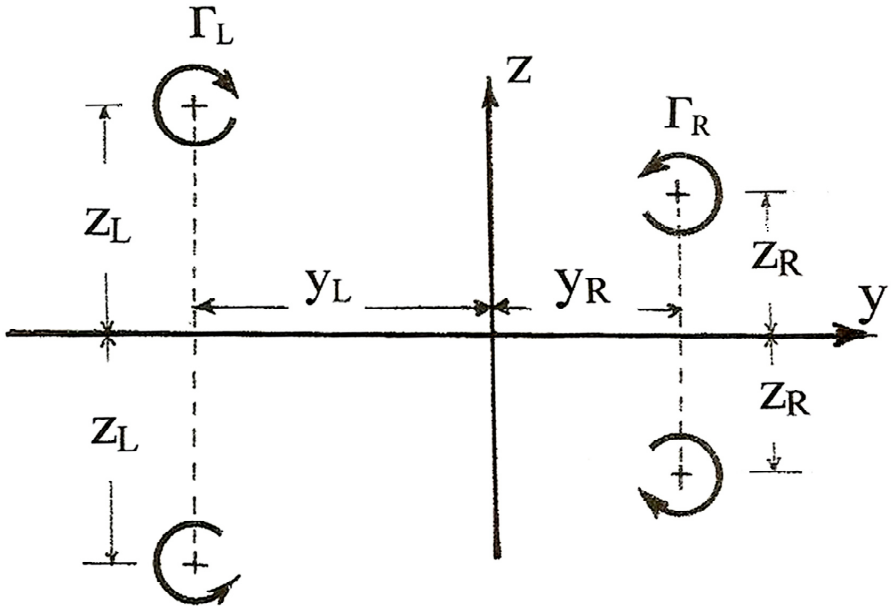

Figure 3. Real and image vortices above and below the ground.

The velocities are determined using a coordinate frame where z denotes the vertical direction, y the lateral direction, and x the direction of the flight. The horizontal and vertical components of the velocity of the R vortex in Fig. 3 are given by:

$$V_y^R = \frac{\Gamma_R}{4\pi Z_r} + \frac{\Gamma_L (Z_r - Z_l)}{2\pi D_1^2} - \frac{\Gamma_L (Z_r + Z_l)}{2\pi D_2^2} \tag{1a}$$

$$V_z^L = \frac{\Gamma_l S}{2\pi D_2^2} - \frac{\Gamma_l S}{2\pi D_1^2} \tag{1b}$$

The horizontal and vertical components of the velocity of the L vortex are given by:

$$V_y^L = -\frac{\Gamma_L}{4\pi Z_l} + \frac{\Gamma_R (Z_r - Z_l)}{2\pi D_1^2} + \frac{\Gamma_R (Z_r + Z_l)}{2\pi D_2^2} \tag{1-c}$$

$$V_z^L = \frac{\Gamma_l S}{2\pi D_2^2} - \frac{\Gamma_l S}{2\pi D_1^2} \tag{1-d}$$

in which S, D_1^2 and D_2^2 are given by (See also Kantha, 1996)

$$S = |Y_L| + |Y_R| \tag{1-e}$$

$$D_1^2 = S^2 + (Z_L - Z_R)^2 \tag{1-f}$$

and

$$D_2^2 = S^2 + (Z_L + Z_R)^2 \tag{1-g}$$

The horizontal components of the velocity ***on the ground*** (directly below the vortices), (sometimes referred to as the 'slip velocity' on the wall) due to all four vortices (two real and two image) are given by

$$V_{z=0}^R = \frac{1}{\pi}\left\{\frac{\Gamma_R}{Z_R} - \frac{\Gamma_L Z_L}{S^2 + Z_l^2}\right\} \tag{2-a}$$

and

$$V_{z=0}^L = \frac{1}{\pi}\left\{-\frac{\Gamma_L}{Z_L} + \frac{\Gamma_r Z_r}{S^2 + Z_r^2}\right\} \tag{2-b}$$

Clearly, the magnitude of the horizontal velocity *along the y-axis* varies with y. The equations for them will not be reproduced here because they will not be needed in the evaluation of the ground effect.

The prediction of the 'rebound' or the motion of vortices in Ground Effect is made as follows:

1. It is assumed that the strengths of the descending vortices and the separation distance b_o between them are known at the time the vortices enter IGE.

2. It is suggested that the calculations begin at Z (the starting value) = 0.54 αb_o where α should be taken as 1.0 (the reasons for it will be explained later).

3. A suitable time interval Δt should be chosen (for a wake that lasts about 100 seconds, $\Delta t = 4$ s may be satisfactory.

4. The components of the horizontal and vertical velocities of the left and right (real and image) vortices are calculated using the equations given above [Eqs. (1-a) through (1-g)].

5. The slip velocity directly below the R and L vortices (i.e., *on the wall*) must be calculated due to all four vortices using the equations given above (Eqs. 2a and 2b).

6. At the very first step ($t = 0$), the vortices (two real and two image) should be moved horizontally for a time interval Δt, i.e., $T = \Delta t$.

7. At the end of the first step, the strength of right-hand vortices (real vortex and its image) should be reduced by $0.5(V^R_{z=0})^2 \beta \Delta t$ and the strength of left-hand vortices should

be reduced by $0.5(V_{z=0}^{L})^2 \beta \Delta t$. For the first set of calculations β should be taken equal to 1.0.

8. The vertical position z of each vortex should be increased by the increment of the displacement thickness, given by

$$\Delta\delta = 0.19\kappa b_o (\Delta T) T^{-(1/3)\lambda} \tag{3}$$

using κ = λ = 1. This relatively simple equation is based on an extensive study of the behavior of turbulent boundary layers in adverse pressure gradients and the analyses governing their variation {see, e.g., Schlichting, 1979 (Seventh Edition)}. Suffice it to note that the literature has been very thoroughly searched for any and all inspiration.

9. In summary, at the end of the first step, one should have a new (reduced) Γ (for both the left and right vortices and their images), a reduced slip velocity (for both the R and L vortices), a new (increased) elevation, and a new time: *T(n) = T(n-1) + ΔT*. Then the above calculations should be applied to move to time 2Δt, so as to arrive at a new set of values of positions, circulations, slip velocities, etc. This process should be continued until the strength of the vortices reduces to about ten percent of their original value.

The reason for the introduction of the 'uncertainty' parameters α, β, κ and λ is to be prepared (at the stage of programming) to deal with the 'vagaries' of nature, ground conditions, and other uncertainties. They should all be taken unity for the first set of calculations (about a dozen or so) for the landing conditions where **there is no wind shear or stratification**. Following a careful analysis of the results, it may be necessary to increase or decrease (hopefully slightly) the values of the said uncertainty parameters.

Representative predictions using the No-Shear/No-Stratification model

Figures 4 and 5 show the comparison of the predictions of the present model with the **3-D LES simulations** of Proctor *et al*. (2000) for two vortex heights (Z = 1, and Z = 0.32). Our predictions and the LES simulations are in reasonable agreement. The position of the *ideal vortices* are also shown for times up to T = 4, but, as noted above, they are not used for $T > 0$.

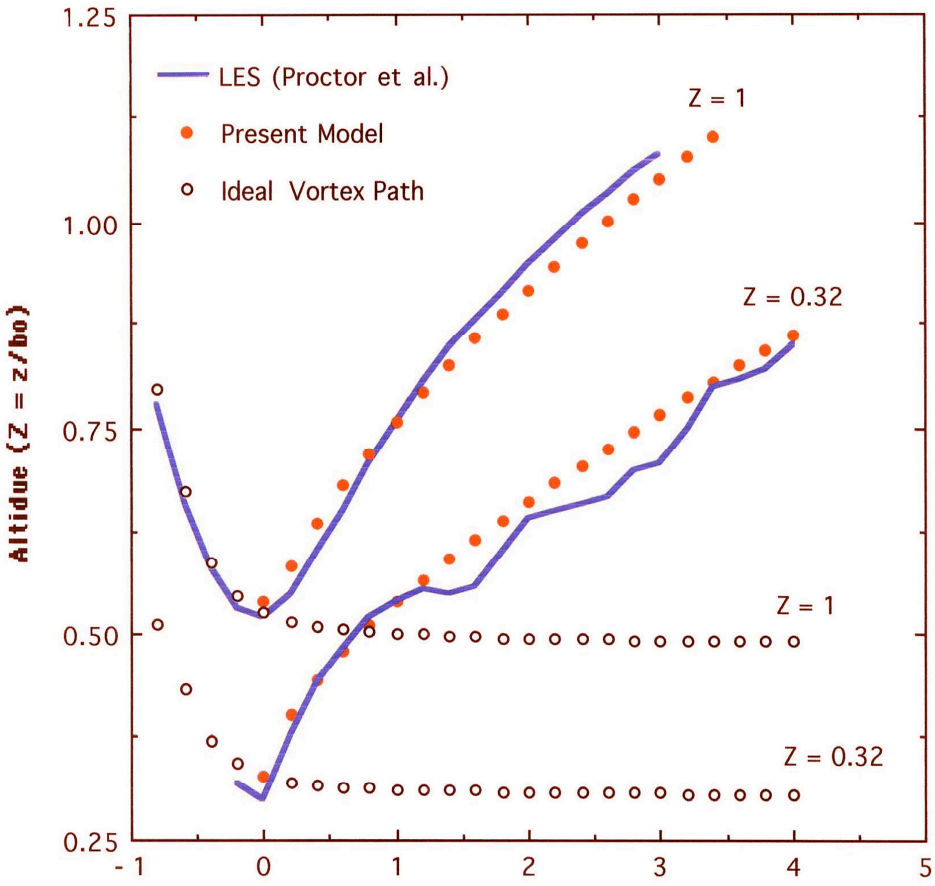

Figure 4. The variation of the vortex altitude with the normalized time T and the comparison of the predictions of the new model with the LES simulations of Proctor, Hamilton and Han (2000).

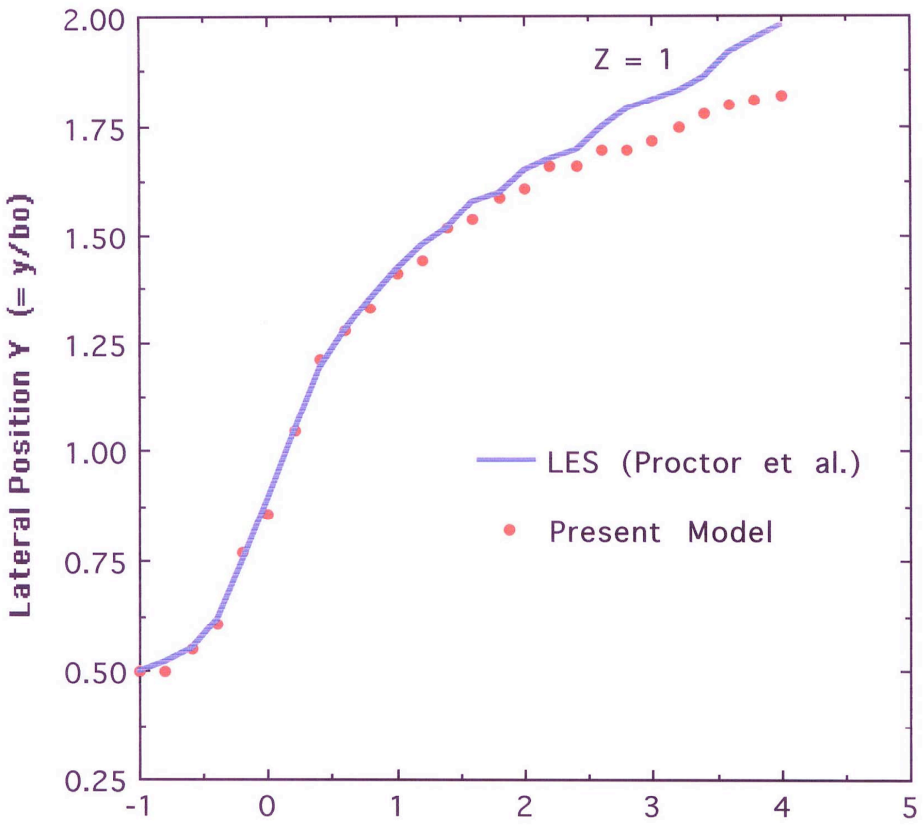

Figure 5. The variation of the lateral position of the vortex with the normalized time T and the comparison of the predictions of the new model with the LES simulations of Proctor, Hamilton and Han (2000).

Figure 5 shows the lateral position of the vortex for $Z = 1$ only. Our predictions for T smaller than about 2.5 are somewhat below those predicted by the LES calculations. This is attributed to several reasons. An artificial *vortex decay model has not been used*. The circulation in our calculations decayed rapidly due to the ground effect (calculated from $\Delta\Gamma = -0.5V_s^2\Delta t$ using the slip velocity V_s on the wall) decreased sharply and was found to be in good agreement with the 3-D LES predictions of Proctor et al. (2000) as evidenced by Figures 4 and 5.

The next example (MEM-1516) is chosen from a field experiment conducted at Memphis International Airport (MEM) by NASA in August 1995. The comparison of the model predictions with the MEM-1516 Lidar measurements (Fig. 6) is not as good as expected for T > 1.5.

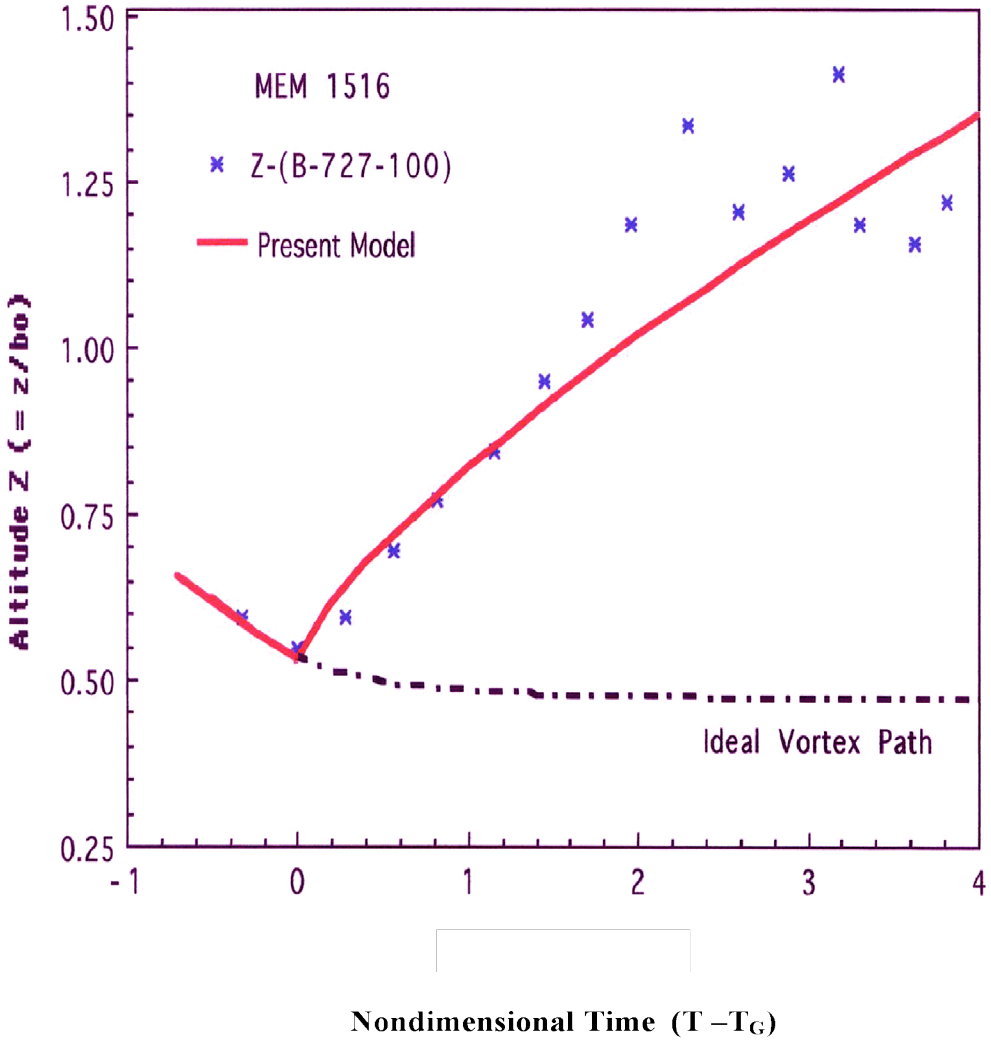

Figure 6. Comparison of the model predictions with the Lidar data of MEM-1516. The dashed line is the path of the ideal vortex.

The (No-Shear, No-Stratification) version of the model does not, as noted previously, deal with the effects of wind, shear, and stratification. Secondly, the vortices of B-727-100 are relatively weak and, as all such weak vortices at larger *T*, are more readily driven by the prevailing atmospheric conditions. Nevertheless, the comparisons of the predictions of a physics-based model with the two cases noted above and the ease with which the effects of wind, shear, and other atmospheric occurrences can be incorporated into it provided sufficient impetus for the development of a more general model.

A GENERALIZED PHYSICS-BASED IGE MODEL

The wind shear and the wake vortices

We begin with the definition of a number of parameters:

(a) A reference to a *Wake Vortex* (WV) refers to all (four) wake vortices and their images, unless otherwise noted (see, Fig. 3). The initial vortex separation is b_o.

(b) A *shear vortex* means one of the relatively small vortices modeling *a segment* ΔZ_i *of the shear layer* in all real and imaginary shear layers extending from the ground to the wake vortices at a given time.

(c) *Mean wind* means the arithmetic mean of the total crosswind velocity from the ground to a WV. Note that it may be different for the Port and Starboard vortices.

(d) *Shear velocity* (U_c) represents the mean of the horizontal velocity at the centroid of a sufficiently small vertical segment ΔZ (see Fig. 7 below).

(e) *Shear parameter* Sh_p for a given segment ΔZ is defined as: $(b_o/V_c)(dV/dz)$ where $V_c = (V_{i+1}+V_i)/2$. The vortex spacing b_o may be replaced by *twice the radius of the peak*

tangential velocity or by the diameter in which the circulation is averaged (see Fig. 7). The elemental vortices representing the shear layer are placed at the centroids of the elements. Their strength, though not identical, does not change with time as long as the wind profile remains steady during the period of landing of the aircraft, i.e., they represent the steady shear in which the WVs are imbedded. This work does not deal with the effects of gust on the wake.

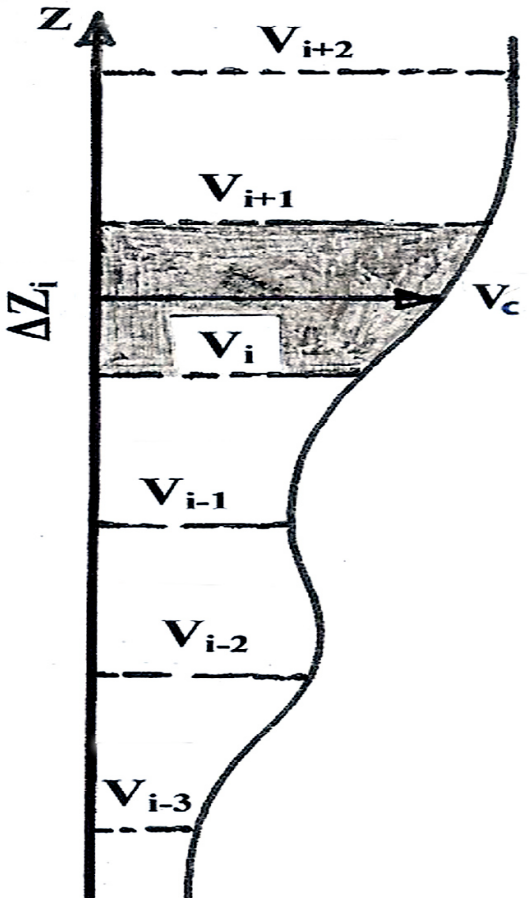

Figure 7. Schematic diagram of a non-uniform shear flow.

V_c is the mean of the shear velocity in the shaded segment.

Even though Sh_p is an important parameter for the definition of the prevailing shear and its magnitude, it does not account for the *lateral variations* of the shear along the vortex. It is a well-known fact that (Proctor *et al.* 2006) steady linear shear is relatively ineffective due to the absence of mixing. The three dimensionality of the shear (or shear volume) accelerates the demise of the oppositely-signed vortex because the *mixing* (one of the most important characteristics of turbulence) and the Eddy-Dissipation Rate are enhanced by non-sinusoidal instabilities, vortex breakdown, and enhanced Eddy Dissipation Rate (Epsilon). Thus, the non-linear shear not only transports the vortices, as in the case of a steady uniform wind but also helps to break them up (at least one) much sooner as in the case of the Idaho Data 757-Run 9. These will need to be studied further in the near future using 3-D LES simulations and physics-based mixing models to account for the accelerated demise of vortices in 3-D unsteady nonlinear shear.

(6) Root-mean-square of V_{sv} : rms(V_{sv}), defined by,

$$rms(V_{sp}) = \left(\frac{1}{N} \sum_{1}^{N} \left(\frac{b_o}{Vavg} \frac{V_{i+1} - V_i}{\Delta z_i} \right)^2 \right)^{1/2} \tag{3}$$

is a good measure of the overall character of the shear layer for a 2-D wind. It can also be evaluated for a *shear volume* if it were possible to obtain reliable data. The larger the rms(V_{sp}), the larger are the nonlinearities in shear. For rms(V_{sp}) smaller than about 0.1, the shear is negligibly small.

Description of the basic steps

The fundamental features of the all-inclusive new model are described below in as much detail as possible:

(1) Ambient potential temperature and crosswind are assumed to be provided at regular intervals.

(2) The rate of change of circulation of the Wake Vortices (and their images) *due to thermal stratification* is calculated in exactly the same manner as given by Greene (1986) and will not be repeated here for sake of brevity. However, it must be noted that for wake vortices out of ground effect and not subjected to environmental winds, a relatively simple model of the vortex decay and transport can be devised successfully (Switzer & Proctor, 2002). They have shown that their *"Large Eddy simulations support the hypothesis that the decay of the vortex hazard is decoupled from its change in descent rate."*

(3) Ambient turbulence is considered to be negligible. However, it can be included (only approximately) with negligible difference in the final predictions). This is because of the fact that the ambient turbulence is a small fraction of the turbulence generated by the wake vortices near the ground. This becomes even more so as the wake vortices come closer and closer to the ground (up to a certain distance). The issue becomes further complicated because the proximity of the real and imaginary wake vortices might give rise to vortex linking.

(4) It is apparent from the foregoing that it is not necessary to use arbitrary *decay rates* and *shear effects*, guesstimated at very time step in the Near Ground Effect region by going *one step backward and two steps forward*, as done by Robins & Delisi (2006).

(5) The rms value of the shear is calculated. If it is below a certain minimum (say, 0.1), shear is ignored and the calculations are performed using only the lateral drift due to uniform crosswind.

(6) If the shear is found to be significant, then the vertical distance between a WV and the ground is divided into N non-equal elements, (N may be as much as 10, depending on the shape of the shear, see Fig. 7). In regions of strong shear smaller distances and in regions of weak shear larger distances should be used. The circulation due to the shear segment at a given N is then assigned to a shear vortex, situated at the centroid of the element. It is noted that then there are 4 WV's (the two at the Starboard side are not necessarily at the same Z as those at the Port side. These lead to 4N shear vortices. Thus, the number and the position of the shear vortices should be judiciously selected to optimize CPU and to enhance the representation.

(7) A remarkable feature of the unusual flow under consideration is that each WV and its image, hovering over the ground, give rise to a fairly uniform velocity profile (within a distance of about $b_o/5$ from the ground), which may be regarded as *new* at each time interval because the lateral speed of the vortex centers ($\Gamma/4\pi Z$) is about a quarter (or less) of the (inviscid) fluid velocity near the ground, ($\Gamma/\pi Z$).

(8) The new velocity of each WV (say WV-4), is calculated using the vectorial sum of all the velocities due to *all* ***shear vortices*** *(of constant strength) and the remaining* WV's [WV(1) through WV(3)]. The same is repeated for each WV. The result is a new set of velocities at each WV. The displacement thickness $\Delta\delta_1$, and the lateral displacement of the WV's at the end of each and every time step ΔT are calculated and the position of each WV are updated.

(9) The circulation decay due to wall friction is calculated from $\Delta\Gamma = -\ 0.5V_S^2\Delta t$ using the slip velocity V_s on the wall (at suitable time intervals, e.g., $\Delta T = 0.4$) and due to the change that comes from the stratification ($-AZN^{*2}$) where A is proportional to the cross-sectional area of the vortex oval (Greene, 1986). Then the circulations of each WV

are calculated anew. Proctor *et al*. (2006) have noted that "For conditions with stable stratification, the mean vortex separation can decrease with time (Switzer & Proctor, 2000) causing the vortex to descend faster than if the separation remained constant." For simplicity, they have assumed the separation of WVs remain constant and empirically modified the Greene's (1986) formulation to $d\Gamma_S^* / dT = -0.42 ZN^{*2.5}$.

(10) The displacement thickness δ_1 of the velocity profile may be calculated using either the existing models on turbulent wall flows or a less complicated physics based model. Here, a power law model is fitted to the boundary layer within $0 < Z_{bl} < 0.12$. For example, for a 1/7 power low model, a typical value of δ_1 is about 0.56 m. The calculations are then continued until the strength of the stronger of the WVs reduces to about 30% of its initial value. The presence of a strongly nonuniform shear could change this percentage and precipitate the earlier demise of one (or both) vortices.

(11) The *lateral positions* of WVs are determined from their successive positions.

The model described above does not use artificial *vortex decay.* The *c*irculation decay due to the ground effect and stratification is fluid-mechanically sound. The preliminary calculations with *no shear and no stratification* produced results (Sarpkaya, 2006) in good agreement with the 3-D LES simulations of Proctor *et al.* (2000). Thus, we have every reason to believe that the general model presented here will prove to be a sound *Physics-based Real-time IGE model of Aircraft Wake Vortices Subjected to crosswind shear, Stratification and Rebound.* As in all such models there is much room for improvement through the infusion of new inspiration from LES simulations, field experiments, and constructive criticisms.

Representative predictions using the generalized model

The comparison of the predictions of the generalized model for MEM-1500 (B727), MEM-1494 (DC-10), and the Idaho Data 757-Run 9 are presented in the following. LES simulations are not available for these field tests.

For MEM-1500, there was a nearly constant shear and relatively small stratification. The temperature has nearly doubled within the region from Z = 15 m to about Z = 40 m and then remained nearly constant. The data for the *port vortices* were not given in the original data. Thus, Figure 8 shows only the data for the Starboard vortex together with the model predictions.

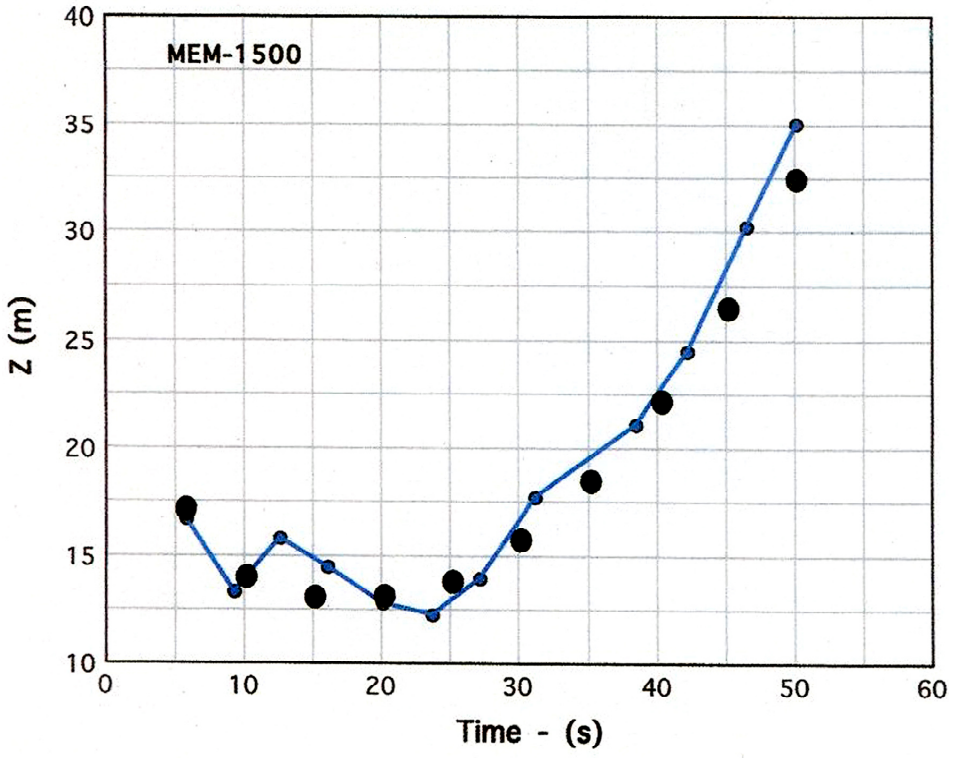

Figure 8. Comparison of the model predictions with the Lidar data of MEM-1500.

For MEM-1494, there was a nearly constant wind shear but the temperature remained nearly constant over a height of about 100 m. The starboard vortex rose nearly steadily up to about T = 60 s and then underwent a dip near T = 60 s, followed by another rapid rise, eventually reaching a nearly constant level at T = 70 s. Figure 9 shows only the Starboard vortex together with the model predictions. Apparently, the data are not sufficient for the model to track the sudden drops and rises of the Starboard vortex. Neither the wind profile nor the temperature profile exhibited any unusual phenomenon to offer a suggestion for the deviation of the Z-data from the model predictions. It appears that there were other reasons or weather conditions, not recorded by the Lidar. The behavior exhibited by MEM-1494 is considered very important for the exploration of the underlying reasons.

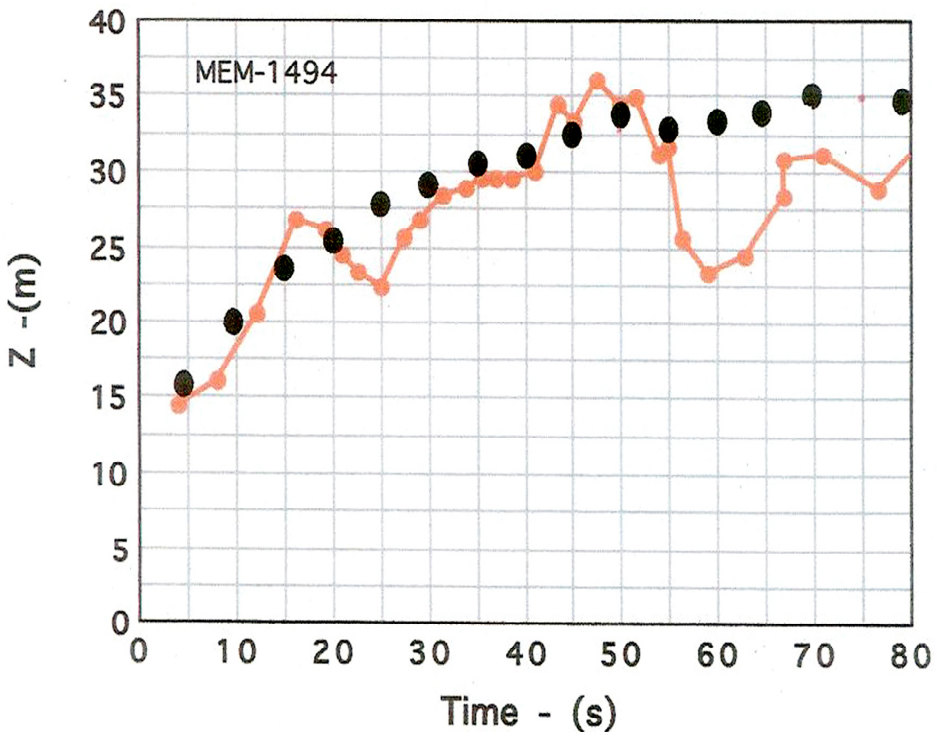

Figure 9. Comparison of the model predictions with the Lidar data of MEM-1494.

For IDAHO-B-757-200 Run 9: The relatively comprehensive data for this benchmark case for the influence of *strong shear* was presented in digital form [Γ = 365 m^2/s, b_o = 30 m, Z(initial) = 70 m, Y(initial) = -95 m (relative to the tower)]. This was extremely helpful in assessing the performance of our model. We will first present the Eddy-dissipation-Rate (Edr, or Epsilon) (Fig. 10a), the temperature (Fig. 10b) and the Crosswind data (10c), and then discuss the behaviors of the Port and Starboard vortices.

Figure 10a shows that the Epsilon values are larger than about 10 cm^e/s^3 from near ground to about 200 m, the top of the tower (h ~ 40 m). This height is nearly at the lowest elevation (35 m) reached by the Starboard (STB) vortex. Thus, for all intents and purposes no Epsilon data is available for the STB vortex. However, and interestingly enough, the Port vortex remains at altitudes below 35 m for which the Epsilon data 'before the wake', 'after the wake', as well as their average, are available. These will not be discussed further for sake of brevity.

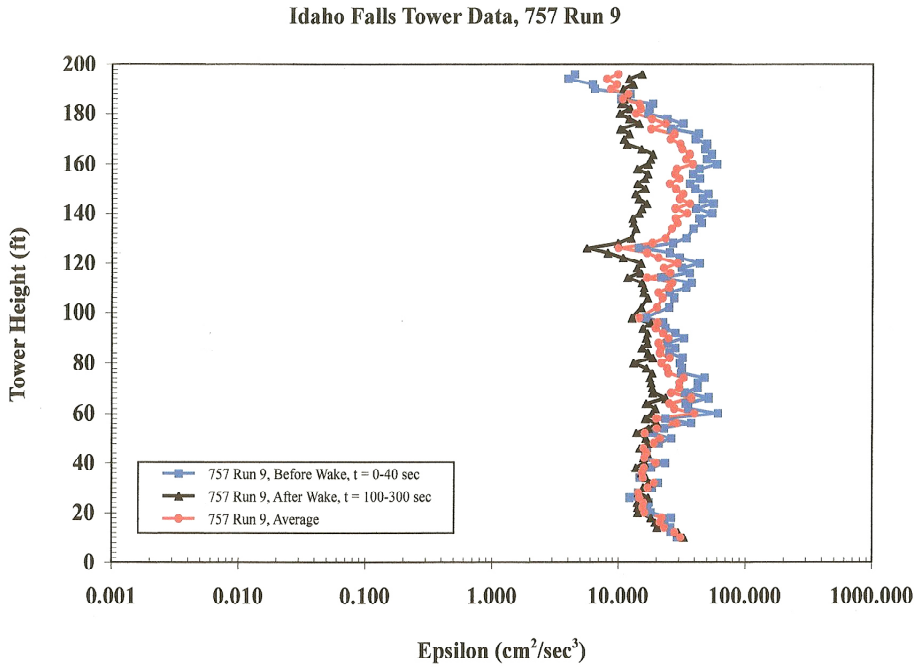

Figure 10a. Epsilon data from the Idaho Falls Towers, 757-Run 9.

Figure 10b shows the strong variation of temperature with elevation. It is interesting to note that the temperature increases rather rapidly within a height of 120m and the STB vortex experiences a temperature increase from about 8^o (at 35 m) to about 10^o (at about 90 m).

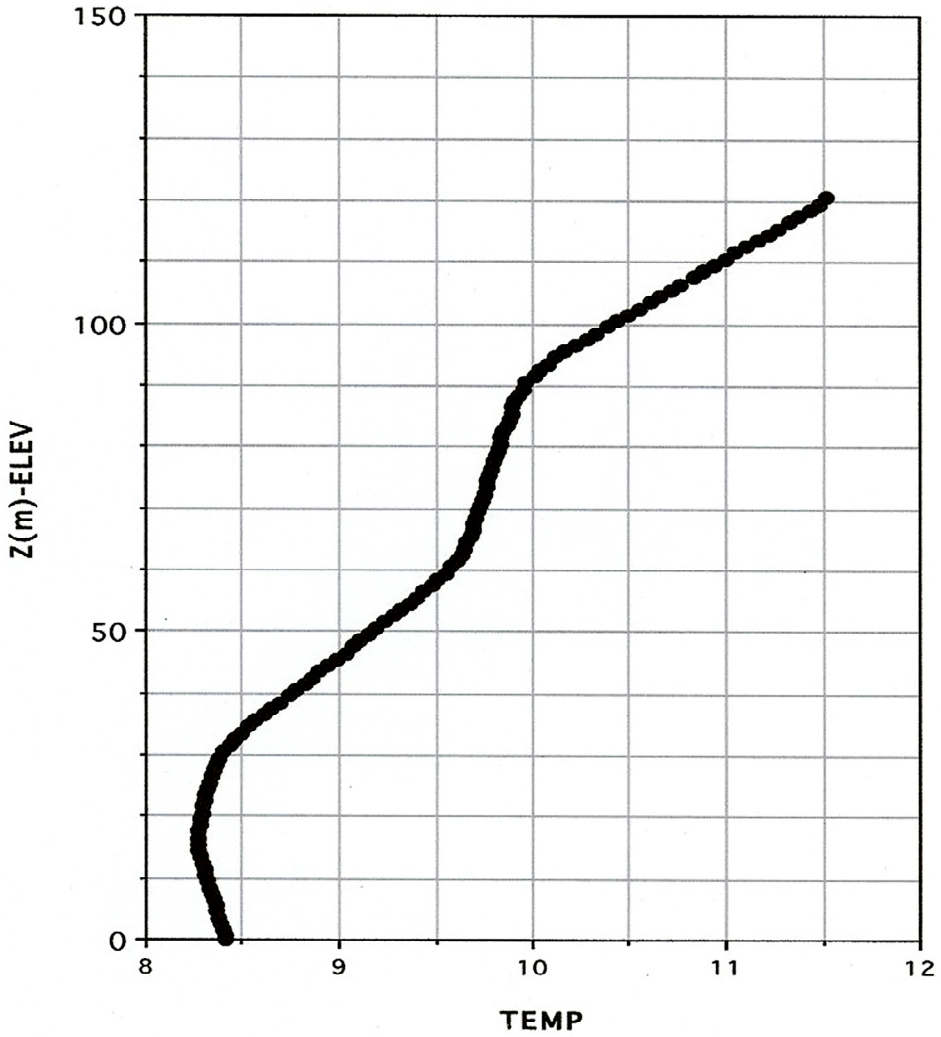

Figure 10b shows the variation of the cross wind with Z. Its absolute value increases rather rapidly from about |3 m/s| (at about 35 m) to |6 m/s| (at about 90 m). This is evident in the lateral motion of both vortices.

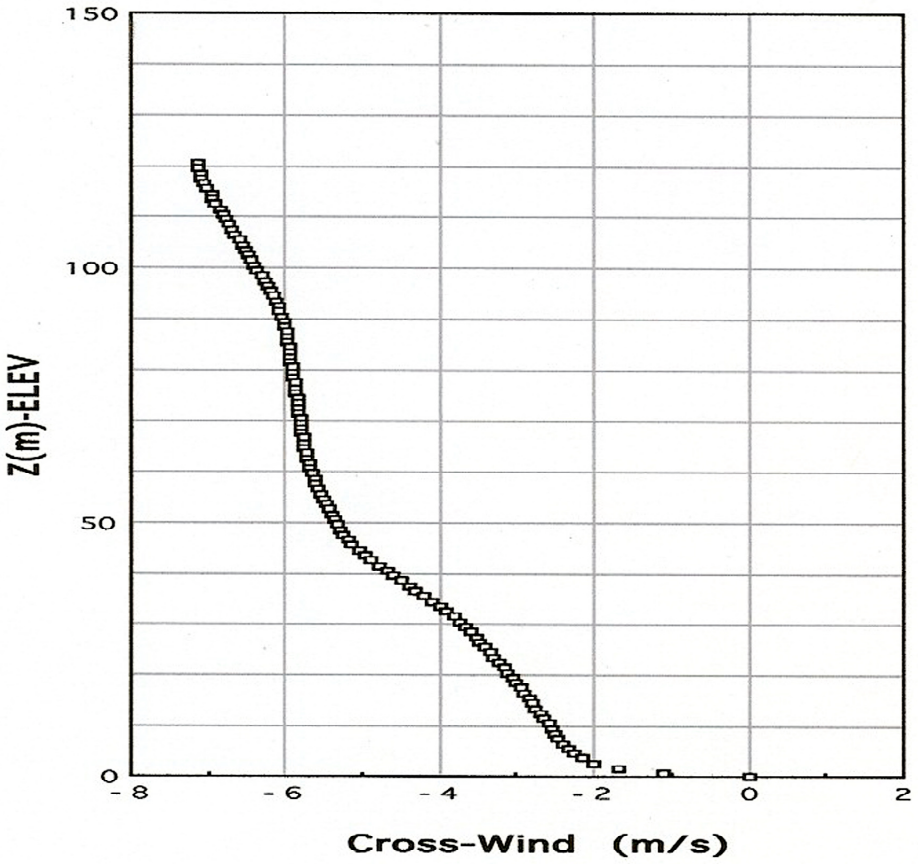

Figure 10c. Variation of the Crosswind with Z.

The variation of the cross wind and the resulting shear are most conducive to the rise of the STB vortex, to relatively small variations in Z, and to occasional fluctuations in the PRT vortex. These are confirmed by our model, as will be discussed later.

Figure 10d shows a plot of both the elevation and lateral position of the STB and PRT vortices. Evidently, the gross difference between the magnitudes of the Z and Y values obscures the finer details of the vertical motion of the vortices within a relatively small elevation.

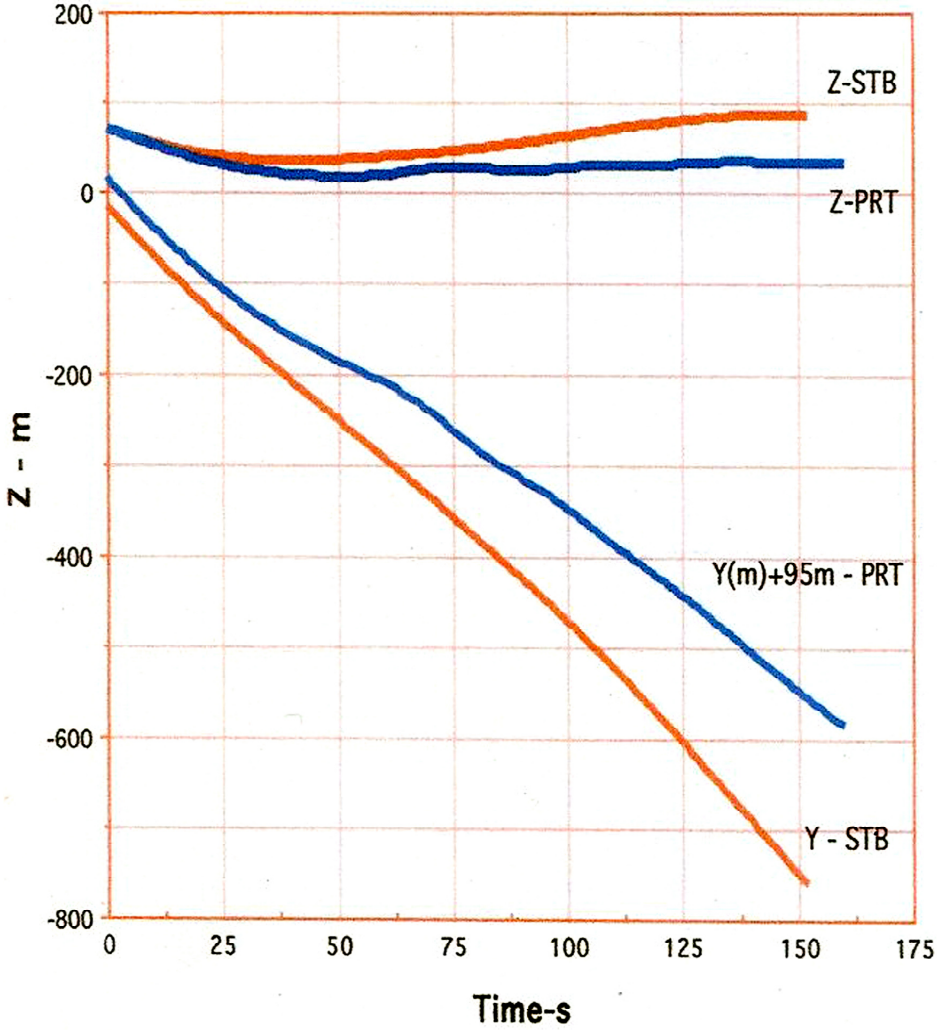

Figure 10d. The Z and Y values of the PRT and STB vortices.

Thus, Fig. 10e is presented below, showing only the Z values of the PRT and the STB vortices and the model predictions (black symbols). The Y values are dealt with in a separate plot.

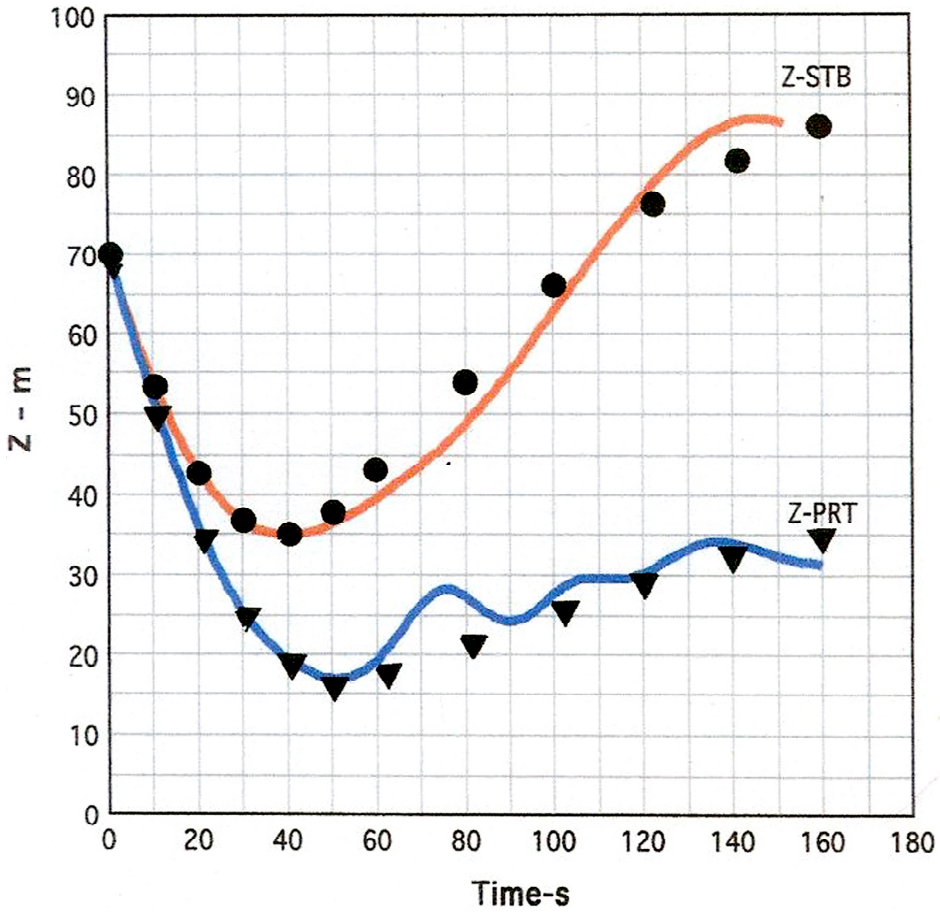

Figure 10e. The elevation versus time of the PRT and STB vortices.

As noted earlier the STB vortex shows large variations following its dip at about T = 40 s, partly due to shear and partly due to stratification. These will be discussed further later.

The measured and predicted lateral motions and circulations of the wake vortices are shown in Figs. 10f and 10g (courtesy of Drs. F. H. Proctor and G. F. Switzer).

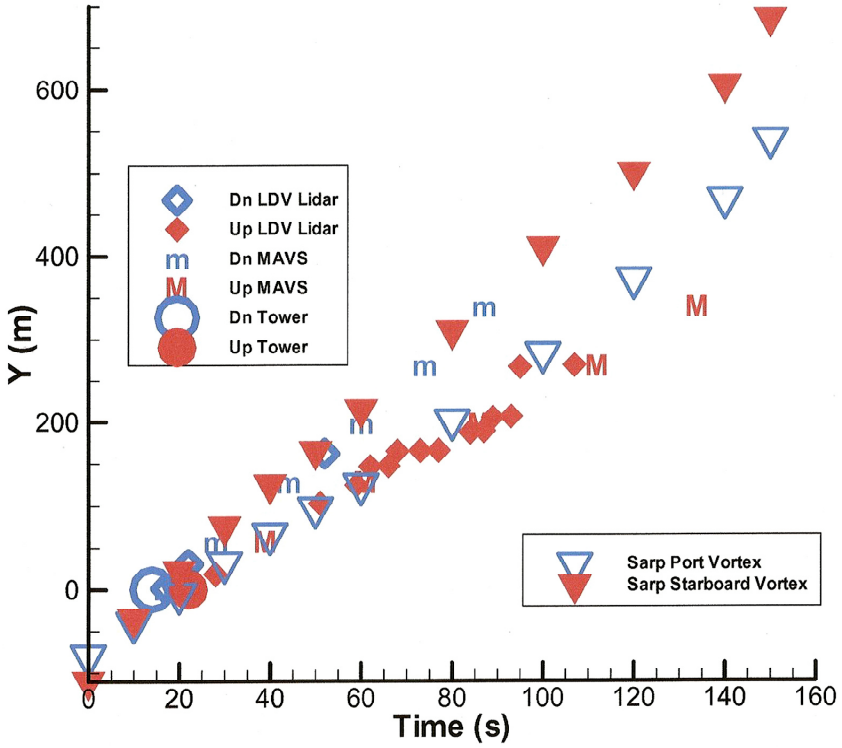

Figure 10f. The comparison of the measured and predicted lateral displacements of the wake vortices.

Figure 10f shows the predicted Y values (white and red triangles) and the field data as a function of time. Two important observations may be made: (a) the agreement between the two sets of data for both the Port and Starboard vortices is fairly satisfactory only for times smaller than about 100 seconds; (b) the strong dominance of the non-linear shear leads, as discussed at length earlier, to strong mixing between the wind shear and the counter-sign vorticity and to the rapid development of lengthwise instabilities and other dissipation mechanisms. These effects have not yet been modeled. The field data will serve as an important guide and provide impetus for the creation of a physics-based **shear-enhanced-demise** sub-model of the wake vortices, particularly for the nonlinear shear. This is left to future modeling efforts and LES simulations of not only of the

IDAHO-B-757-200 Run 9 but also of additional data with strong nonlinear shear. It also appears that the demise of the wake vortices be further categorized (e.g., due to vortex breakdown, prevailing atmospheric turbulence, wind with no shear, wind with shear of varying intensity, etc.) for a better understanding of the physics of the problem and more confident modeling. It appears that dumping all of our ignorance into one parameter we call 'damping' is an unnecessary restriction that can reduce accuracy and applicability.

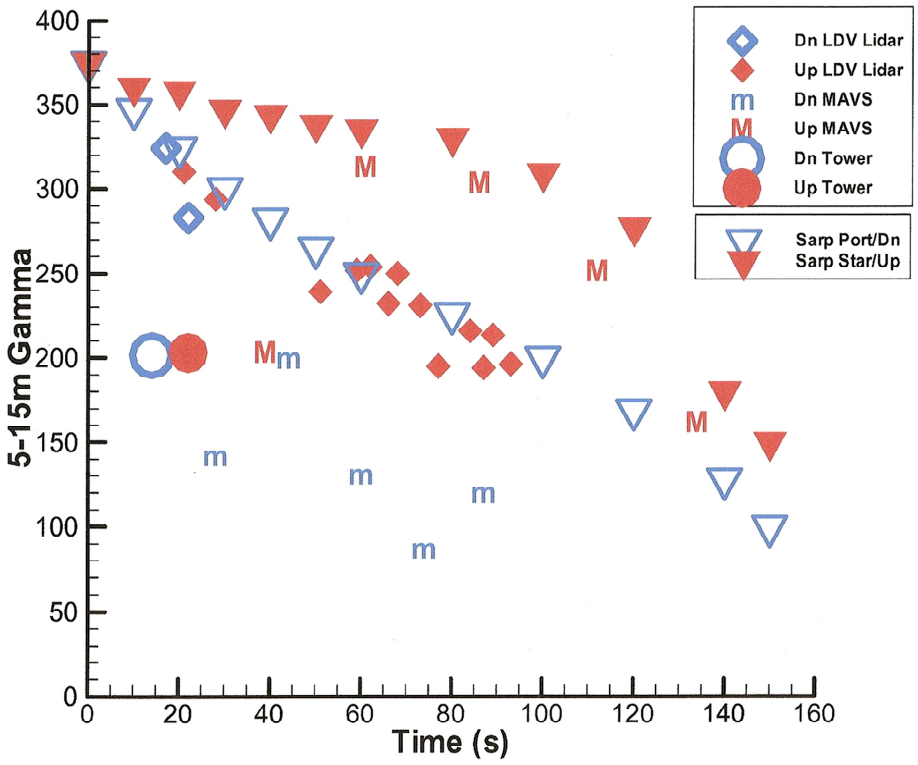

Figure 10g. The comparison of the measured and predicted (5-15m) circulations of the wake vortices.

Figure 10g shows the decrease of circulation. The comments made on the lateral displacement of the vortices apply equally well to the decay of the vortices. In other

words, all aspects of the demise of wake vortices, excluding those that do not involve shear and/or stratification, need to be re-examined (e.g., slow-decay versus sharp-demise). These in turn will lead to a better modeling of the mechanisms that control their persistence or their untimely demise. Empirical formulations and hand waving need to give way to the evolution of physics-based models, particularly for 'operational models.'

DISCUSSION OF RESULTS AND CONCLUSIONS

The reduction of the separation of the leading and following aircrafts is desirable to enhance the airport capacity provided that there is a physics-based operational model applicable to all regions of the flight domain (out of ground effect, OGE; near ground effect, NGE; and in ground effect, IGE) and that the quality of the quantitative input from the measurements of the prevailing atmospheric conditions and the quality of the total airport operations regarding the safety and the sound interpretation of the prevailing conditions match the quality of the analysis and numerical simulations.

This report deals only with the creation of a physics-based real-time IGE model of the aircraft wake vortices subjected to crosswind, stratification and shear. The comparison of the model predictions with the Large Eddy Simulations (LES) and with the existing field data has been rather encouraging. However, it gave rise to a number of fundamental questions which can only be resolved and incorporated into our model through additional field tests, observations, and the development of 'intelligent' and 'physics based' demise mechanisms. The model described herein is a first step towards these objectives and, when asymptotically perfected, should smell far more physics and far less curve fitting.

REFERENCES

Greene, G.C. (1986) "An Approximate Model of Vortex Decay in the Atmosphere". Journal of Aircraft, Vol. 23, No. 7, pp. 566-573.

Hofbauer, T. & Gerz, T. (1999) "Effects of nonlinear shear on the dynamics of a counter-rotating vortex pair," 1st Int'l Symposium on Turbulence and shear flow phenomena, 12-15 Sept., Santa Barbara, CA.

Hofbauer, T. & Holzäpfel, F. (2003) "Behavior of Aircraft Wake Vortices Subjected to Wind Shear." AIAA-2003-3813.

Holzäpfel, F. (2003) "Probabilistic Two-Phase Wake Vortex Decay and Transport Model." Journal of Aircraft, Vol. 40, No. 2, March-April, 2003.

Kantha, L. H. (1996) "Empirical Model of Transport and Decay of Wake Vortices Between Parallel Runways." Journal of Aircraft, Vol. 33, No. 4, July-August 1996

Proctor, F. H. & Han, J. (1999) "Numerical Study of Wake Vortex Interaction with the Ground Using the Terminal Area Simulation System." AIAA-99-0754.

Proctor, F.H., Hamilton, D.W., & Switzer, G.F. (2006) "TASS Driven Algorithms for Wake Prediction." AIAA-2006-1073.

Proctor, F.H., Hinton, D.A., Han, J., Schowalter, D.G., & Lin, Y.-L. (1997) "Two Dimensional Wake Vortex Simulations in the Atmosphere: Preliminary Sensitivity Studies." AIAA-97-0056.

Proctor, F.H., Hamilton, D.W, & Han, J. (2000) "Wake Vortex Transport and Decay in Ground Effect: Vortex Linking with the Ground." AIAA-2000-0757.

Robins, R.E. & Delisi, D.D. (2006) "Modeling Crosswind Shear Effects in NASA's AVOSS Prediction Algorithm." AIAA-2006-1076.

Sarpkaya, T. (2000) "A New Model for Vortex Decay in the Atmosphere." Journal of Aircraft, Vol. 37, No. 1, pp. 53-61.

Sarpkaya, T. (2004) "A Critical Review of the Transport and Decay of Wake Vortices in Ground Effect." 'In Ground Effect' Workshop Presentations: WakeNet USA [CD-Rom], New Orleans, April 27-29.

Sarpkaya, T. (2006) "Towards the creation of a Physics-Based Ground Effect Model." AIAA-2006-1072.

Suponitsky, V., Cohen, J., & Bar-Yoseph, P.Z., (2004) "Evolution of Localized Vortex Disturbance in Uniform Shear Flow: Numerical Investigation." *AIAA J.*, Vol. 42, No. 6, pp. 1122-1131.

Switzer, G.F. & Proctor, F. H. (2002) "Wake Vortex Prediction for Decay and Transport within Stratified Environments." AIAA-2002-0945.

Zheng, Z.C. & Baek, K. (1998) "Inviscid Interactions Between Wake Vortices and Shear Layers." J. Aircraft, Vol. 36, pp: 477-480).